Analytica Chimica Acta 1126 (2020) 91–99

Contents lists available at ScienceDirect

Analytica Chimica Acta

journal homepage: www.elsevier.com/locate/aca

Low fouling strategy of electrochemical biosensor based on chondroitin sulfate functionalized gold magnetic particle for voltammetric determination of mycoplasma ovipneumonia in whole serum

Shiyi Zhao [a], Yingxia Zhou [a], Lai Wei [a], Lihua Chen [a, b, *]

[a] Key Laboratory of Optic-electric Sensing and Analytical Chemistry for Life Science, Shandong Key Laboratory of Biochemical Analysis, Key Laboratory of Analytical Chemistry for Life Science in Universities of Shandong, Key Laboratory of Eco-chemical Engineering, College of Chemistry and Molecular Engineering, Qingdao University of Science and Technology, Qingdao, 266042, PR China
[b] Kashijinhuitong Industrial Development Co., Ltd, Kashi, 844000, PR China

HIGHLIGHTS

- Based on a novel antifouling nanomaterial, a sensitive sensor for MO was constructed.
- This novel biosensor for MO can directly detect the related disease markers in whole serum.
- It is one of few successfully-constructed electrochemical biosensors for MO.

GRAPHICAL ABSTRACT

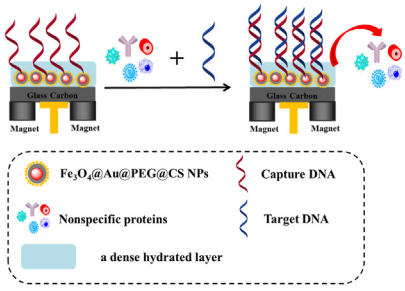

ARTICLE INFO

Article history:
Received 26 March 2020
Received in revised form
10 May 2020
Accepted 8 June 2020
Available online 18 June 2020

Keywords:
Antifouling
Biosensor
Goat serum
Magnetic beads
DPV

ABSTRACT

Based on the successful design and preparation of Fe_3O_4@Au@polyethylene glycol (PEG)@chondroitin sulfate (CS) nanoparticles, a novel electrochemical biosensor was elaborately developed for MO determination by the drop coating method. This biosensor demonstrates ultra-low fouling properties in complex biological systems, especially in whole serum. Only 2.40% of the differential pulse voltammetry (DPV) signal changes are shown in the resistance test of electrode interface to 100% goat serum. The constructed biosensor also presented a good selectivity (DNA samples for M1, M2 and M3give a response around 14.2–21.4%of that obtained by the target analyte), reproducibility (the relative standard deviation (RSD) is only 4.82%) and storage stability (93.2% of the initial response is maintained after 20 day). Moreover, this biosensor exhibits high analytical performance with a wide line arranges (10^{-17} M ~ 10^{-12} M) in buffer, even in 100% goat serum. In both cases, a low limit of detection (LOD) of 3.3

* Corresponding author. Key Laboratory of Optic-electric Sensing and Analytical Chemistry for Life Science, Shandong Key Laboratory of Biochemical Analysis, Key Laboratory of Analytical Chemistry for Life Science in Universities of Shandong, Key Laboratory of Eco-chemical Engineering; College of Chemistry and Molecular Engineering, Qingdao University of Science and Technology, Qingdao, 266042, PR China.
E-mail address: Lihuachen@qust.edu.cn (L. Chen).

https://doi.org/10.1016/j.aca.2020.06.015

aM(S/N = 3)is showed. To our knowledge, a few examples reported the application of electrochemical biosensors to the direct ultrahigh sensitive determination of MO, especially in whole serum.

1. Introduction

Mycoplasma ovipneumonia (MO), a highly infectious disease, can spread silently at the herd level [1]. When it is found, there is no any therapeutic significance from the perspective of economic profit ability. One of the most effective means to prevent the outbreak of MO still is its early diagnosis. Currently, several elegant methods, including isolation culture method [2], electron microscopy [3], serological methods [4], loop-mediated isothermal amplification (LAMP) [5], polymerase chain reaction (PCR) method [6] and fluorescence method [7] have been widely reported and applied.

However, these traditional assays still suffer from these problems of cross reactions, false positives or false negatives, time consuming, the dependence of sophisticated and expensive equipment and the requirement of the strict experimental conditions and the skillful operators. For example, pathogen separation is the “gold standard” for MO, but it usually takes up to two weeks for microbiological culture of MO. EILSA reduces the need for time consuming, but some false positive and negative finding and its relatively complex manipulation greatly limit its application in remote mountainous areas. Thus, developing a point of care, facile and sensitive determination for MO is highly desirable. The problem of the bottleneck in real-time determination of MO is that the disease markers with the extremely low concentration are surrounded by a large number of organic compounds, enzymes and proteins in bodily fluid at the early stage of infection [8].

Electrochemical biosensors as an emerging technology demonstrated its attractive potential in bioassays, due to its low cost, rapid response and high selectivity, especially its excellent sensitivity (10^{-19} M) [9,10]. Recently, this technology is getting more attention because of its successfully application in 100% body fluids (blood, urine and serum) for the determination of the disease [11]. However, to the best of our knowledge, the electrochemical sensors related to MO have seldom been investigated.

The behavior of the excellent electrochemical sensors is influenced by three key factors: the electrical conductivity, the further chemical modification ability and the antifouling ability [12]. The magnetic particles covered with a gold nano-shell are widely used in electrochemical sensors due to its excellent electrical conductivity, the further chemical modification ability and the stability [13,14].

Here, Fe_3O_4@Au NPs are selected as the interface material of the modified electrodes. Nevertheless, in the detection of real biological samples, a lot of active sites on the surface of gold bring a great challenge on the biofouling resistance. Polyethylene glycol (PEG) and chondroitin sulfate (CS) are respectively modified on the surface of Fe_3O_4@Au nanoparticles to improve it. Then, the successfully fabricated Fe_3O_4@Au@PEG@CS NPs were magnetically adsorbed onto the magnetic glassy carbon electrode (MGCE). Interestingly, this novel material endow electrode interface with the excellent low fouling characteristics in a single protein, especially in the complex biological systems. Finally, the specific DNA fragments only representing MO were designed and anchored on Fe_3O_4@Au@PEG@CS NPs modified biosensor and the various properties of the electrode were studied in detail by DPV. This sensor shows a good analytical performance, a wide linear range and the low detection limit for MO assays.

2. Materials and methods

2.1. Chemicals

Hexa ammine ruthenium (III) chloride ($Ru(NH_3)_6^{3+}$) and 1,4-butanediol diglycidyl ether (BDE) were supplied by Sigma-Aldrich (https://www.sigmaaldrich.com/china-mainland.html). Potassium ferricyanide (III), potassium ferrocyanide (II) trihydrate, sodium phosphate dibasic dodecahydrate, sodium phosphate monobasic dehydrate, bovine serum albumin (BSA, MW: 66.43 kDa), sodium bicarbonate, sodium carbonate anhydrous, sodium chloride, hyaluronic acid (HA) and potassium chloride were bought from Aladdin science and technology (China) Co., Ltd (Shanghai) (https://www.aladdin-e.com/). PEG terminated with amino group (molecular weights of 5000 g moL^{-1}) was bought from Shanghai Yare Biotech, Inc (https://guide21901.guidechem.com/) and CS was bought from Shanghai yuanye Biological technology Co., Ltd (http://www.shyuanye.com/). Goat milk was from Shandong Yangchun Sheep Milk Dairy Co., Ltd. It was purchased in the local market and contained 2.8 g protein per 100 g goat milk. The outer membrane protein 31 of brucellosis (OMP31) was donated by college of animal science and technology, Shihezi University. Goat serum was obtained from Shanghai Sangon Biotechnology Co. Ltd (Shanghai, China) (https://www.sangon.com/). All oligonucleotide sequences were synthesized and purified by high performance liquid chromatography (HPLC) at Shanghai Sangon Biotechnology Co. Ltd (Shanghai, China) (https://www.sangon.com/). The sequences of the oligonucleotides are listed in Table S1.

All solutions were prepared with Millipore water from Milli-Q water purifying system. All reagents were analytical grade without further purification and all experiments were taken at room temperature. Buffer includes the phosphate buffered saline (PBS, 10 mM, pH 7.4) and carbonate buffer (CBS, 10 mM, pH 10.56 and pH 9.5).

2.2. Apparatus

Electrochemical measurements (cyclic voltammetry (CV), DPV) were done with the help of a CHI 660E electrochemical workstation from Shanghai CH Instruments Co. Ltd. (China) (http://www.chinstr.com/). A conventional three-electrode system, MGCE (3.0 mm in diameter) as a working electrode, platinum wire as a counter electrode (CE) and saturated calomel as a reference electrode (RE), was utilized in all experiments. The MGCE has three components, a copper connector, a hollow cylinder magnet and a poly tetra fluoroethylene cylindrical tube packed with glassy carbon. CVs were recorded between −0.6 V and 0.2 V using $Ru(NH_3)_6^{3+}$ as probe.

Transmission electron microscopy (TEM) was performed utilizing a JEM-2100 TEM instrument (Hitachi High-Technology Co., Ltd. Japan). Scanning electron microscopy (SEM) images and energy dispersive spectrometer (EDS) were performed with field emission SEM (JEOL JSM-7500F, Hitachi High-Technology Co., Ltd., Japan). Fourier transform infrared spectroscopy (FTIR) was performed with the BRUKER. Water contact angle measurement was recorded using

the JC2000 goniometer of Zhongchen Digital Technical Co. (Shanghai, China).

2.3. Preparation of CS coated magnetic nanoparticles

Fe_3O_4@Au@PEG@CS NPs were successfully synthetized as shown in Scheme.1A (The detail synthesis and characterization of Fe_3O_4@Au NPs are described in the Electronic Supplementary Material S2 and Fig. S1). Then 4-arm−NH_2−PEG (10 mL, 2 mM) was first added into the Fe_3O_4@Au NPs (10 mL, HCl, pH 3) and this mixture was sonicated for30 min and kept static at 4 °C for 48 h. After the water wash treatments, the unreacted PEG in the freshly synthetized Fe_3O_4@Au@PEG NPs solution is removed (Characterization of Fe_3O_4@Au@PEG NPs is shown in the Electronic Supplementary Material S3 and Fig. S2). Subsequently, CS (20 mg, in 2.5 mL water) was mixed with EDC (80 mg) and NHS (80 mg) for 30 min. Then, this mixture was dropped into the solution of Fe_3O_4@Au@PEG NPs (2.5 mL, 10 mg L^{-1}) for another three days of incubation. Finally, the successfully synthesized Fe_3O_4@Au@PEG@CS NPs were collected and then diluted 60 folds with deoxygenated water for further use. The preparation of Fe_3O_4@Au@PEG@HA NPs is the same as that of Fe_3O_4@Au@PEG@CS NPs.

2.4. Preparation of Fe_3O_4@Au@PEG@CS NPs/MGCE

Fe_3O_4@Au@PEG@CS NPs (30 μL) were dropped on the electrode surface. Then this electrode was placed in an oven at 37 °C for 4 h. Finally, the water wash treatment was used to remove the free Fe_3O_4@Au@PEG@CS NPs for the further use. The preparation of Fe_3O_4@Au@PEG@HA NPs/MGCE is the same as that of Fe_3O_4@Au@PEG@CS NPs/MGCE.

2.5. Low fouling performance of Fe_3O_4@Au@PEG@CS NPs modified sensor

A single protein (BSA or OMP31) and the complex media (DNA mixture, 100% goat milk and 100% goat serum) were employed to evaluate the antifouling property of Fe_3O_4@Au@PEG@CS NPs modified sensor. The concentrations of BSA and OMP31 were 10 mg mL^{-1} and 1 μg mL^{-1}, respectively. DNA mixture consisted of three kinds of DNA with same concentration (0.1 μM) (DNA sequences were supported in Table S1). Finally, Fe_3O_4@Au@PEG@CS NPs modified sensor was separately incubated in the above solution, 100% goat milk and 100% goat serum for 30 min and the DPV responses of the electrode before and after incubation were recorded. By the way, the DPV responses of Fe_3O_4@Au@PEG@HA NPs/MGCE before and after incubation in 100% goat serum were also recorded.

2.6. Immobilization of probe DNA

The electrode modified with Fe_3O_4@Au@PEG@CS NPs was immersed in 300 μL BDE (0.6 M, diluted with 10 mM CBS, pH 10.56) for 18 h. After the water wash treatments, 30 μL CBS (10 mM, pH 9.5) containing 1 μM probe DNA (Electronic Supplementary Material S5) was dropped onto the surface of electrode for another 18 h. At last, the MGCE/Fe_3O_4@Au@PEG@CS NPs/probe DNA was thoroughly rinsed with PBS (10 mM, pH 7.4) and stored in PBS at 4 °C before use.

2.7. Electrochemical determination of DNA

Various concentrations of target DNA (30 μL, from 10^{-17} M to 10^{-12} M) were respectively dropped on the modified electrodes and then those electrodes were stored at 37 °C for 45min. The DPV peaks before and after hybridization between probe and target were collected. DPV measurements were performed with a

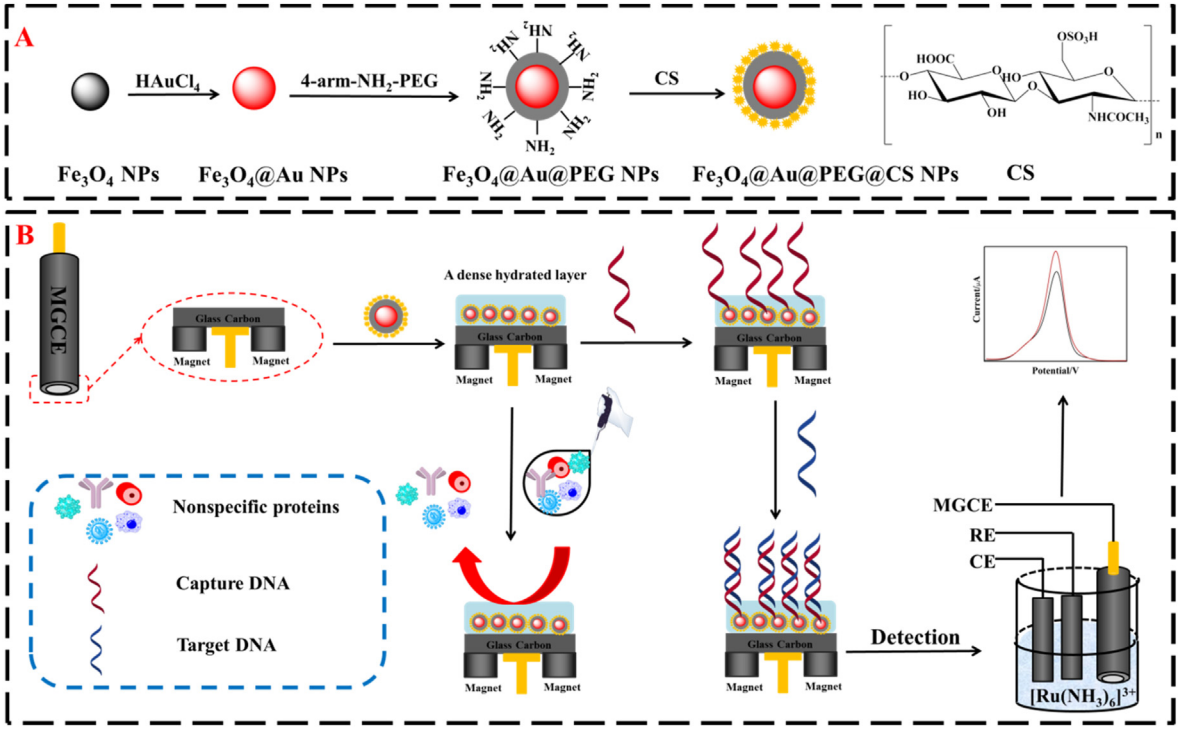

Scheme 1. Illustration of the fabrication of Fe_3O_4@Au@PEG@CS NPs (A); Illustration of the fabrication of low fouling biosensor of Mycoplasma ovipneumonia (B).

potential increment of 4.0 mV, a pulse width (modulation time) of 50 ms, and a pulse amplitude of 50 mV by scanning the potential from −0.6 V to 0.2 V in PBS (10 mM, pH 7.4) doped with 5.0 mM $Ru(NH_3)_6^{3+}$ and 0.1 M KCl. All analyses were performed in triplicate.

3. Results

3.1. The choice of materials and the modified chemistry of Fe_3O_4@Au@PEG@CS NPs based biosensor

Excellent surface of electrode has the properties of a high electrical conductivity, the further chemical modification and the low-fouling. Fe_3O_4@Au NPs modified on interface of electrode endow MGCEs with a good conductive effect [15]. But a large amount of charges at the interface of golden shell will cause strong nonspecific binding in real sample analysis. How to reduce this bio-fouling is one of the most important issues for the construction of sensor interface PEG [16], zwitterionic polymers [11], peptide [17] and glycosaminoglycan [18] as the antifouling material have been widely used in various fields. Thus, PEG terminated with four arms NH_2 was firstly anchored on Fe_3O_4@Au NPs surface by Au−N bond. The C−O−C backbone of PEG can easily form a dense hydrated layer to protect the surfaces of the golden shell from bio-fouling. The density of PEGylation plays a key role in the protein-repellent nature of PEG. But the curvature of the NPs does not allow PEG to form a tight molecular alignment layer on Fe_3O_4@Au@PEG. Thus, another material should be chosen to make up for this shortage.

Chondroitin sulfate (CS), one of the natural glycosaminoglycans, is composed of repeating disaccharide units, including (1−3)-β-D-glucuronic acid and the sulfated Nacetylgalactosamine. The massive amide (CO−NH) and hydroxyl (OH) groups are also the important functional groups for increasing the strength of hydration because of their strong proton accepting ability. So it is modified on the surface of Fe_3O_4@Au@PEG nanoparticles by the addition of EDC and NHS. The carboxyl groups from CS molecules react with EDC/NHS to produce an active ester (O-acylisourea) leaving group. They can more effectively covalently bond to the primary amine of PEG to form a peptide bond on the surface of Fe_3O_4@Au@PEG NPs.

As shown in Scheme.1B, the successfully fabricated Fe_3O_4@Au@PEG@CS NPs were magnetically adsorbed onto the MGCE. Subsequently, in study of the resistance to bio-fouling (Fig. 3), this electrode demonstrates the ultralow-fouling properties towards a single protein, especially towards the complex biological systems. For the electrodes before and after the incubation in 100% goat serum, the percent change of DPV current response is only 2.40% (Fig. 3 D). This is obviously lower than that of the electrode constructed with Fe_3O_4@Au@PEG NPs and Fe_3O_4@Au (Fig. S3). They directly imply that CS can greatly improve the antifouling ability of interface.

Then, the specific DNA fragments terminated with NH_2 only representing MO are fixed on Fe_3O_4@Au@PEG@CS NPs modified biosensor with homobifunctional cross linker, namely, 1,4-butanediol diglycidyl ether (BDE). This cross linker has two reactive groups that are identical in structure and have the same reaction specificity [19]. One epoxy functional group at the end of BDE reacts with amino groups of DNA, and another with hydroxyl group of CS. Subsequently, various DNA hybridization experiments were carried out and ideal results were got.

3.2. Characterization of Fe_3O_4@Au@PEG@CS NPs

To confirm the successful synthesis of Fe_3O_4@Au@PEG@CS NPs, HR-TEM, SEM, FTIR and EDS were used to characterize those nanoparticles. Both TEM (Fig. 1A) and SEM (Fig. 1B) demonstrate that the surface morphology of Fe_3O_4@Au@PEG@CS NPs is spherical with an average diameter of about 169 nm and no aggregation takes place. Surface functional groups of Fe_3O_4@Au@PEG@CS NPs were characterized by FTIR. The spectrum of Fe_3O_4@Au@PEG@CS NPs in Fig. 1C exhibits several characteristic peaks. They are basically consistent with that of Fe_3O_4@Au@PEG NPs (Fig. S2B), excepts for the peak at 800 cm^{-1}. The characteristic peak at 800 cm^{-1} actually corresponds to C−O−S stretching vibration and it only comes from chondroitin sulfate [20]. The EDS spectra of Fe_3O_4@Au@PEG@CS NPs (Fig. 1D) also shows S element from chondroitin sulfate, besides Fe, Au, O, N and C from Fe_3O_4@Au@PEG (Fig. S2C). These indicate the successful synthesis of Fe_3O_4@Au@PEG@CS NPs.

3.3. Electrochemical characterization of the fabrication process of the DNA sensor

The voltammetry is a relatively common method in electrochemical sensors [21]. As shown in Fig. 2, DPV and CV are employed to monitor and characterize the fabrication procedure of the biosensors. In Fig. 2A, DPV current response of the MGCE is first recorded (curve a). When Fe_3O_4@Au@PEG@CS NPs is dripped on the electrode surface (curve b), a significant improvement in the peak currents is gained. It can be attributed to the excellent electrical conductivity of magnetic nanomaterial and the increases of electrode surface area. After the immobilization of probe DNA, a large number of negative charges from DNA phosphate backbone are accumulated on the electrode surface and produce the strong electrostatic attraction to the electrochemical probe carrying positive charge. It results in a dramatic increase of the peak current (curve c). Finally, the target DNA hybridizes with probe DNA (curve d) and the increased negative charges attract more $Ru(NH_3)_6^{3+}$ redox probes to diffuse toward the electrode surface, then the DPV peak current further increases. As can be seen, the result from CV (Fig. 2B) is in a good agreement with that from DPV, further guaranteeing the successful fabrication of the biosensor.

3.4. Low fouling performance of Fe_3O_4@Au@PEG@CS NPs modified biosensor

ITOs modified with and without Fe_3O_4@Au@PEG@CS NPs are immersed into 100% goat serum for 1 h. Then, SEM is used to characterize the morphology of two samples before and after the incubation with 100% goat serum and demonstrates a clear difference each other (Fig. 3A). For ITO modified without Fe_3O_4@Au@PEG@CS NPs, the significant serum levels of substance is shown before and after the incubation with 100% goat serum (Fig. 3A: a and b). However, for ITO modified with Fe_3O_4@Au@PEG@CS NPs, the morphology remains basically unchanged before and after the incubation with 100% goat serum (Fig. 3A: c and d).

The low-fouling performance of electrode interface is closely related to the wettability of the interface [22]. Therefore static contact angle was used to characterize the hydrophilicity of electrode surface. Fig. 3B (contact angle images) and Fig. 3C (contact angle value) show the changes in contact angle for the different nano-layer of electrodes. The water contact angle of Fe_3O_4@Au@PEG NPs modified ITO (about 57.8°) is smaller than that of bare ITO (about 63.6°). After the conjugation of CS with Fe_3O_4@Au@PEG NPs, a large amount of −OH and C−O−C group significantly improved the wettability of nanomaterial. So the contact angle of Fe_3O_4@Au@PEG@CS NPs modified ITO immediately drops to 15.4°.

The better the hydrophilicity of interface is, the higher the surface energy is. The surface energy of each nano-layer of electrode is determined by the sessile drop method. Fe_3O_4@Au@PEG@CS NPs modified ITO with the best hydrophilicity has the

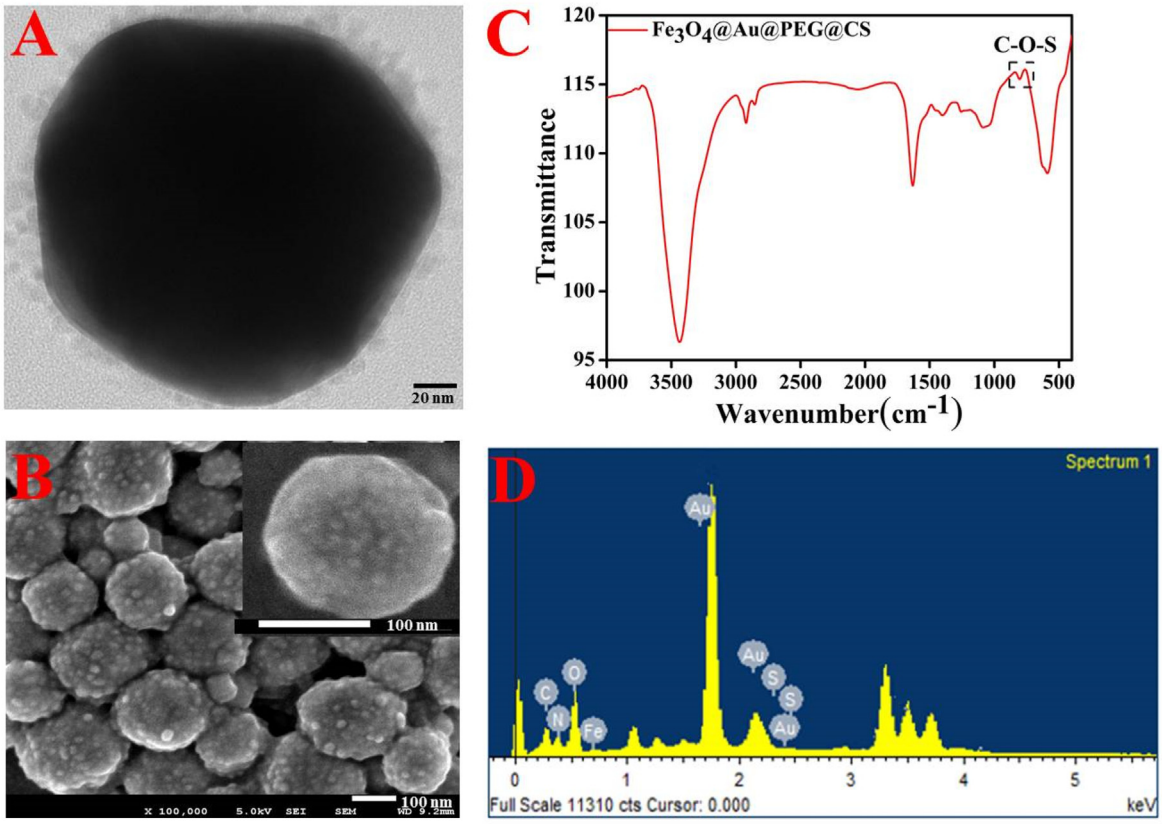

Fig. 1. HR-TEM image of Fe_3O_4@Au@PEG@CS NPs (A); SEM images of Fe_3O_4@Au@PEG@CS NPs (Inset: magnified SEM images ofFe_3O_4@Au@PEG@CS NPs) (B); FTIR spectra (C) and EDS spectra (D) of Fe_3O_4@Au@PEG@CS NPs.

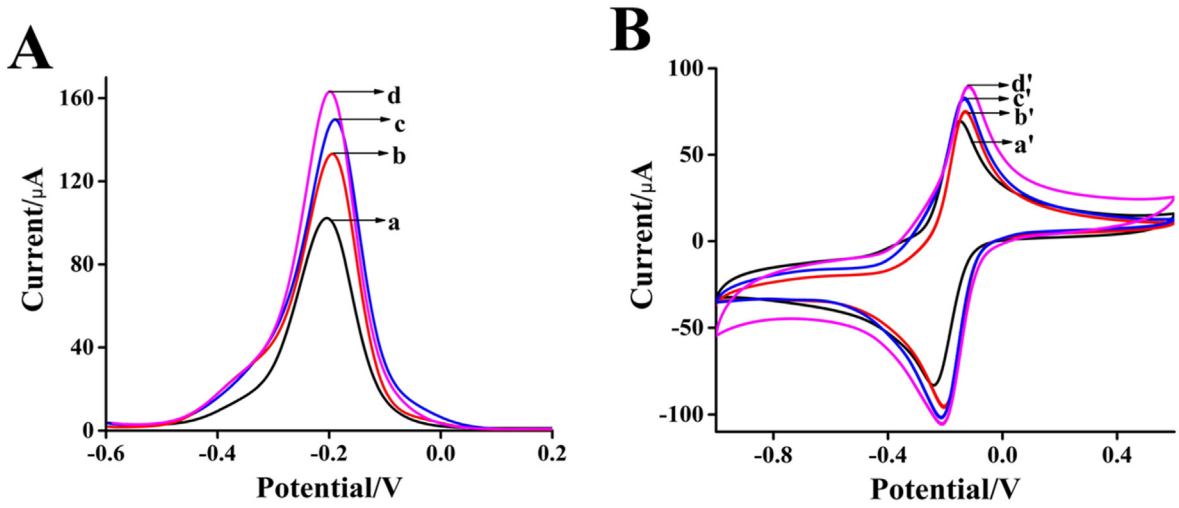

Fig. 2. DPV (A)and CV (B) recorded in PBS (10 mM, pH 7.4) solution containing 5.0 mM $Ru(NH_3)_6^{3+}$ and 0.1 M KCl: (a) (a') bare MGCE; (b) (b') MGCE/Fe_3O_4@Au @PEG@CS NPs; (c) (c') MGCE/Fe_3O_4@Au@PEG@CS NPs/probe DNA; (d) (d') MGCE/Fe_3O_4@Au@PEG@CS NPs/probe DNA/target DNA. DPV and CV signals were respectively detected at potential range from -0.6 to +0.2 V and - 0.8 to +0.4 V.

highest surface energy (Fig. S5). Both the excellent hydrophilicity and the high surface energy of Fe_3O_4@Au@PEG@CS NPs are favorable for the formation of hydration layer which can effectively resist bio-fouling. It is the main reason why Fe_3O_4@Au@PEG@CS NPs has the best antifouling performance.

To make more detailed evaluation on the antifouling performance of the Fe_3O_4@Au@PEG@CS NPs modified electrode, the solution with a single protein (BSA and OMP31) or the complex biological system (DNA mixture, 100% goat milk and 100% goat serum) were used. The current changes of the electrodes before and after the incubation in the different solution were recorded by DPV. DPV value of the electrodes modified with Fe_3O_4@Au@PEG NPs and Fe_3O_4@Au@PEG@CS NPs are first compared. As shown in Fig. S3, the electrodes modified with Fe_3O_4@Au@PEG@CS NPs show

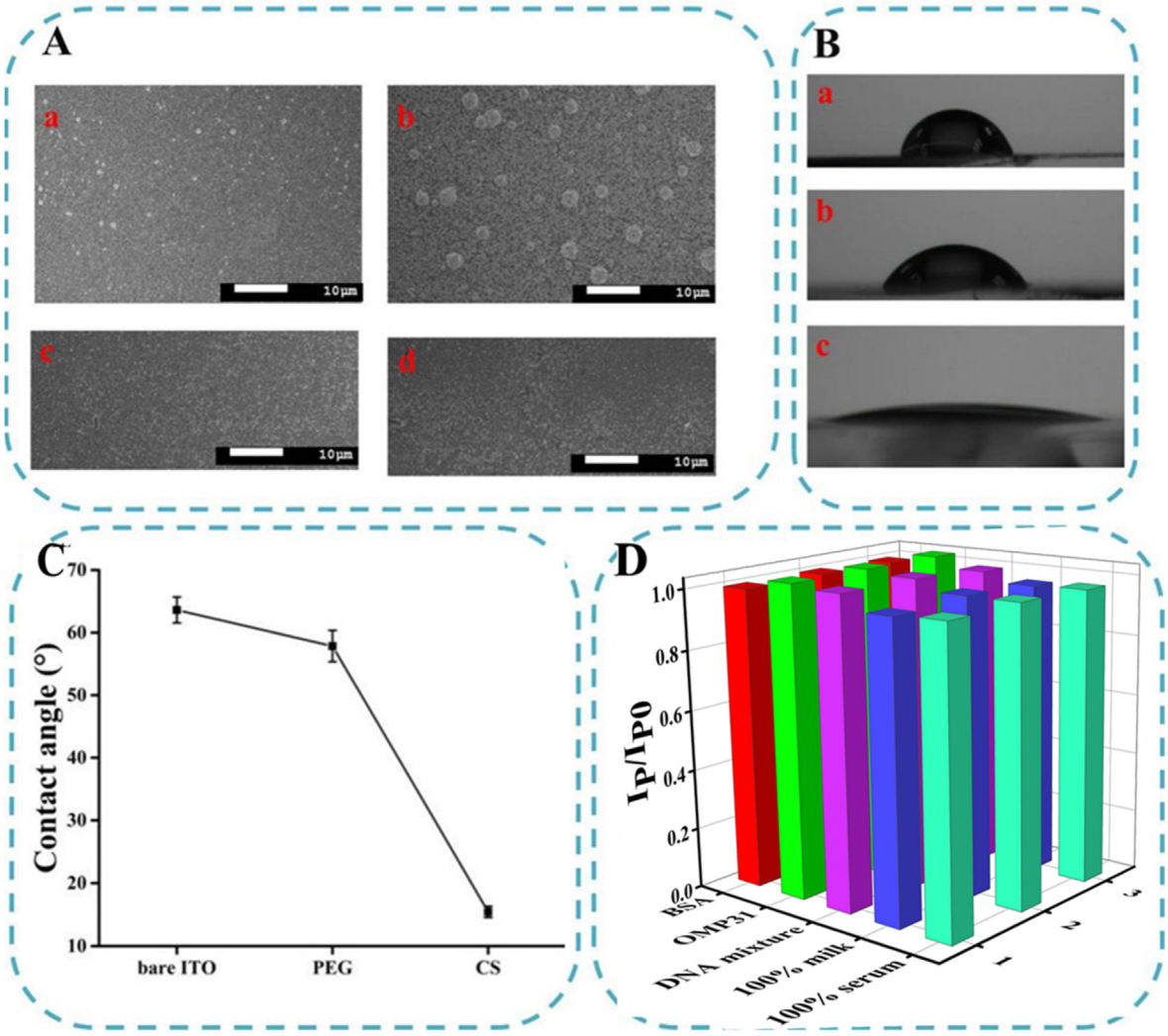

Fig. 3. (A) SEM images of ITO modified without Fe_3O_4@Au@PEG@CS NPs before (a) and after (b) soaked in 100% goat serum, SEM images of ITO modified with Fe_3O_4@Au@PEG@CS NPs before (c) and after (d) in 100% goat serum; (B) Contact angle images of bare ITO (a), Fe_3O_4@Au@PEG NPs modified ITO (b) and Fe_3O_4@Au@PEG@CS NPs modified ITO (c); (C) Contact angle value of bare ITO, ITO/Fe_3O_4@Au@PEG NPs (PEG) and ITO/Fe_3O_4@Au@PEG@CS NPs (CS). (D) DPV responses changes of Fe_3O_4@Au@PEG@CS NPs modified MGCE after incubation in single protein solution (10 mg mL^{-1} BSA and 1 μg mL^{-1} OMP31) and complex media (0.1 μM DNA mixture, 100% goat milk and 100% goat serum), 1, 2 and 3 were the three results of parallel experiments, respectively. DPV measurements were performed in5.0 mM $[Fe(CN)_6]^{3-/4-}$ with a scanning potential from - 0.2 to + 0.6 V.

significantly smaller DPV value changes before and after immersing in 100% goat serum. They confirm our expectation that the fusion of CS can effectively improve the antifouling ability of nanomaterial. Fig. 3D exhibits that the changes of DPV current (Ip/Ip0) caused by the nonspecific adsorption of electrode interface from BSA (10 mg mL^{-1}), OMP31 (1 μg mL^{-1}), DNA mixture (0.1 μM), 100% goat milk and 100% goat serum are 0.99, 1.03, 1.02, 0.98 and 0.976, respectively. Obviously, the fluctuations of current value are very minor. These strongly confirmed that Fe_3O_4@Au@PEG@CS NPs can endow the electrode interface with an excellent antifouling property again. By the way, the antifouling ability of Fe_3O_4@Au@PEG@HA NPs is similar to that of Fe_3O_4@Au@PEG@CS NPs. CS can be replaced by HA (Fig. S6).

3.5. MO target response on the MGCE/Fe_3O_4@Au@PEG@CS NPs/probe DNA in buffer or in 100% serum

In order to achieve optimal electrochemical response, incubation time is optimized for the probe/target DNA interaction [23]. MGCE/Fe_3O_4@Au@PEG@CS NPs/probe DNA was immersed into target DNA solution (1.0×10^{-9} M) at 37 °C for the different incubation times (15 min up to 60 min). The DPV response increases with the elongation of incubation time and then reaches nearly constant in 45 min (Fig. S7). Thus, 45 min is chosen as the optimal incubation time for the following experiments.

The electrochemical analytical performance of Fe_3O_4@Au@PEG@CS NPs/probe DNA modified electrode for the determination of MO was studied in PBS containing various concentrations of target DNA by DPV. As shown in Fig. 4A, the current responses of the biosensor increase along with the increasing concentration of the target DNA (10^{-17} M -10^{-12} M). It confirms the successful formation of DNA double helix between the probe and the target. The percentage of DPV current changes [ΔIp/Ip0 (%)] is linearly related with the logarithm of the concentration of the target DNA in the range from 10^{-17} M to 10^{-12} M with the limit of detection of 3.3 aM (S/N = 3) (as seen in Fig. 4B). The linear regression equation is [ΔIp/Ip0 (%)] = 59.43 + 3.31 lgC, and the correlation coefficient (R^2) is 0.9983. Interestingly, when the same experiment is carried out in 100% goat serum, a good linear correlation ([ΔIp/Ip0 (%)] = 59.15 + 3.29 lgC, R^2 = 0.996, Fig. 4C) and a low limit of

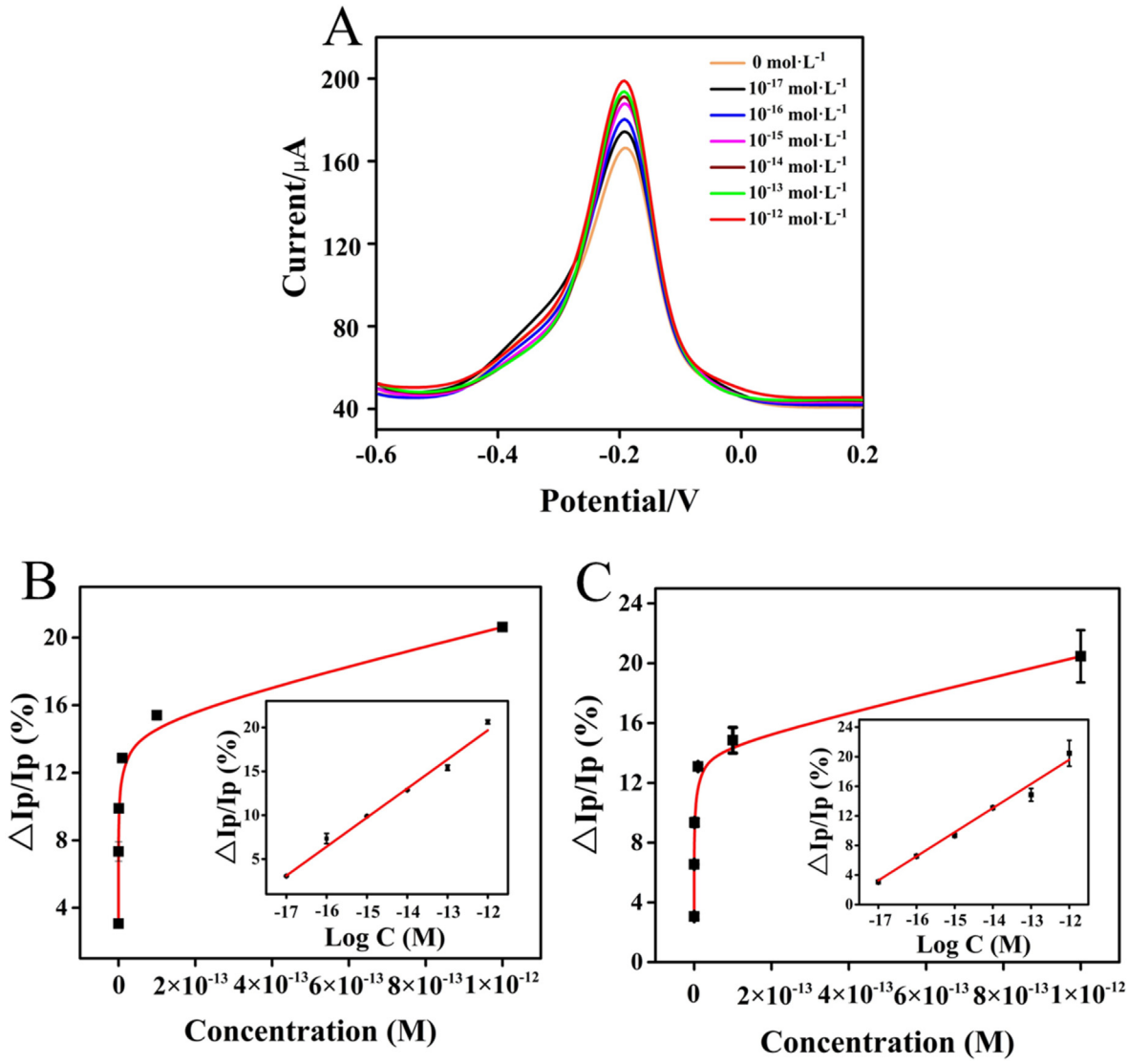

Fig. 4. DPV response curve of the biosensor to different concentrations of target DNA in PBS (A); Dynamic response range and calibration plot (inset) of the biosensor against target DNA concentration in PBS (B) or in 100% goat serum (C). DPV measurements were performed 5.0 mM $Ru(NH_3)_6^{3+}$ with a scanning potential from - 0.2 to + 0.6 V.

detection (LOD) (3.3 aM, S/N = 3) are still exhibited. To be sure, compared with others, this novel biosensor has its own unique advantages (as shown in Table 1).

3.6. Selectivity, reproducibility and stability of MO biosensor

To assess the selectivity of the biosensor, the current response [ΔIp/Ip0 (%)] of the biosensors was respectively measured in various solutions (WB-DNA, M1-DNA, M2-DNA, M3-DNA and Target DNA). As shown in Fig. 5, compared with the current response [ΔIp/Ip0 (%)] to target DNA, the current response to WB-DNA, M1-DNA, M2-DNA and M3-DNA is smaller, although concentrations of WB-DNA, M1-DNA, M2-DNA and M3-DNAare 1000-fold higher than that of target DNA. The excellent selectivity may be

Table 1
Comparison of different magnetic material.

Method	Magnetic material	Substance to be examined	Linear range	Detection limit	Media	References
Electrochemistry	Ag@MWCNT-IL-Fe_3O_4	Glucose oxidase	6 μM- 2 mM	2.12 μM	In buffer	[27]
Surface enhanced Raman scattering	GO wrapped Fe_3O_4@Au	Nile blue A	–	0.1 nM	In buffer	[28]
Electrochemistry	Fe_3O_4@Au	MON810 maize gene	0.25–2.5 nM	0.15 nM	In buffer	[29]
Resonance light scattering	Fe_3O_4@Au	Alzheimer's amyloid-β peptide (Aβ)	5.0 fM - 5.56 nM	1.2 fM	In buffer	[30]
Electrochemistry	Fe_3O_4@Au-GSH	Estradiol	0.025 μM - 10.0 μM	2.76 nM	In buffer	[15]
Electrochemical biosensor	Streptavidin-magnetic beads	Tuberculosis	1 aM - 1 fM	0.5 aM	In buffer	[31]
Electrochemistry	Fe_3O_4@SiO_2nanoparticles	Acetaminophen (AP)	60 nM - 50 μM 50 μM - 200 μM	17.3 nM	In buffer	[32]
Electrochemistry	Fe_3O_4@Au@PEG@CS NPs	Mycoplasma pneumoniae	10 aM-0.1 nM	3.30 aM	In whole serum	Present assay

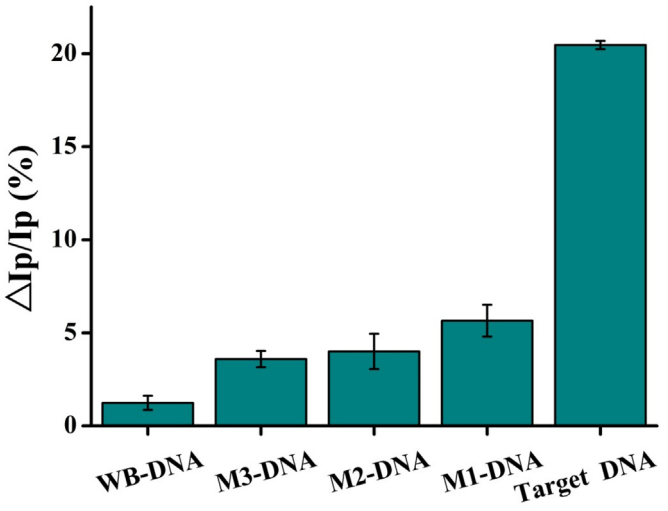

Fig. 5. DPV responses change of the biosensor to target DNA (1.0×10^{-12} M) and WB-DNA, M1-DNA, M2-DNA and M3-DNA (1.0×10^{-9} M) respectively.

interpreted as the integrated results of the low fouling property of the sensor and the strong bioaffinity between probe DNA and target DNA.

The reproducibility of the electrochemical MO biosensor is evaluated using five independent electrodes modified with Fe_3O_4@Au@PEG@CS NPs/probe DNA and 10^{-12} M target DNA was used in this experiment (Fig. S8). Under the same conditions, the relative standard deviation (RSD) was only 4.82% and this indicates the good reproducibility of the biosensor.

Stability is a very significant factor for the practical applicability [24]. One case is that the biosensor constructed by He et al. retained 92.6% signal in 10 days [25]. Another case is the biosensor designed by Xie et al. retains 91.3% of its initial current response after 15 days [26]. The long term stability of MGCE/Fe_3O_4@Au@PEG@CS NPs/probe DNA/target DNA is assessed by monitoring the response of DPV current (Fig. S9). After the storage in the PBS solution in a refrigerator at 4 °C for 5 days, the response of DPV current are held constant. For 14 day, it still retains approximately 93.6% of the initial response. After 20 day, it drops to 93.2%. Compared with the reported work, this biosensor has better stability. Such excellent stability of the biosensor can be attributed to chemical stability of materials (Fe_3O_4@Au@PEG@CS NPs). They provide friendly micro-environment to maintain DNA bioactivity.

3.7. Analytical performance of biosensor in 100% goat serum

The biosensors were also used to detect MO in 100% goat serum by standard addition method in order to investigate the practical application of the designed biosensor. Target DNA was added into 100% goat serum and this mixture was shook for 2 min for the preparation of the target DNA with the different concentrations (1.0×10^{-17} M – 1.0×10^{-14} M). Then, they were, respectively, dropped on MGCE@Fe_3O_4@Au@PEG@CSNPs@Probe DNA for 45 min at 37 °C. After water washing treatment, those electrodes were separately putted into a three-electrode system and performed in PBS (10 mM, pH 7.4) doped with 5.0 mM $Ru(NH_3)_6^{3+}$ and 0.1 M KCl. DPV is used to record electrochemical signals by scanning the potential from −0.6 V to +0.2 V. Finally, the concentration (Found) of MO was obtained by formula [ΔIp/Ip0 (%)] = 59.15 + 3.29 lgC. The recovery results as shown in Table S2 are in the range of approximately 102% and 106%, with RSD between 0.38% and 4.49%. Determination of the low concentrations of DNA in 100% goat serum is very important for the early diagnosis of disease.

4. Conclusions

A selective electrochemical biosensor for the highly sensitive determination of MO was elaborately designed and constructed based on the successful preparation of Fe_3O_4@Au@PEG@CS NPs. CS as a new antifouling material conjugating with Fe_3O_4@Au@PEG NPs endows the electrode surface with near perfect low-fouling properties in various biological media. Therefore, in the hybridization between probe DNA only representing MO and target DNA, a very good selectivity is demonstrated in a wide range of determination (10^{-17} M-10^{-12} M) in buffer, even in whole serum and a very low limit of detection are also gained. To our knowledge, it is one of the few successfully constructed electrochemical sensors about MO so far. It is more encouraging that this sensor achieves the goal of direct determination of disease in whole serum. But this modified electrode also has its own limitations. Magnetic nanoparticle is easy to agglomerate when stored for a long time, so after the preparation, this novel material should be used immediately to ensure the optimal effect of the electrode.

CRediT authorship contribution statement

Shiyi Zhao: Investigation, Methodology, Software, Data curation, Writing - original draft. **Yingxia Zhou:** Visualization, Investigation. **Lai Wei:** Supervision, Software, Validation. **Lihua Chen:** Conceptualization, Methodology, Writing - review & editing.

Declaration of competing interest

The authors declare that they have no known competing financial interests or personal relationships that could have appeared to influence the work reported in this paper.

Acknowledgments

This work was supported by the Joint Funds of the National Science Foundation of China (U1303283). National High Technology Research and Development Program of China (2015AA034602). The science and technology project and achievement transformation plan of modern agricultural of Xinjiang Corps (2016AC010). The National Science and Technology Major Project (2017YFD0500304) and science and technology branch project of Xinjiang autonomous region science and technology project to support Xinjiang autonomous region (2018E02021).

Appendix A. Supplementary data

Supplementary data to this article can be found online at https://doi.org/10.1016/j.aca.2020.06.015.

References

[1] D. Xue, Y. Ma, M. Li, Y. Li, H. Luo, X. Liu, Y. Wang, Mycoplasma ovipneumoniae induces inflammatory response in sheep airway epithelial cells via a MyD88-dependent TLR signaling pathway, Vet. Immunol. Immunopathol. 163 (1–2) (2015) 57–66, https://doi.org/10.1016/j.vetimm.2014.11.008.

[2] Y.C. Lin, R.J. Miles, R.A. Nicholas, D.P. Kelly, A.P. Wood, Isolation and immunological detection of Mycoplasma ovipneumoniae in sheep with atypical pneumoniaand lack of a role for Mycoplasma arginini, Res. Vet. Sci. 84 (3) (2008) 367–373, https://doi.org/10.1016/j.rvsc.2007.06.004.

[3] A. Al-Kaissi, M.R. Alley, Electron microscopic studies of the interaction between ovine alveolar macrophages and Mycoplasma ovipneumoniae in vitro, Vet. Microbiol. 8 (6) (1983) 571–584, https://doi.org/10.1016/0378-1135(83)90006-8.

[4] M. Giangaspero, R.A. Nicholas, M. Hlusek, B. Bonfini, T. Osawa, R. Orusa, S. Tatami, E. Takagi, H. Moriya, N. Okura, K. Kato, A. Kimura, R. Harasawa,

R.D. Ayling, Seroepidemiological survey of sheep flocks from Northern Japan for Mycoplasma ovipneumoniae and Mycoplasma agalactiae, Trop. Anim. Health. Prod n. 44 (3) (2012) 395–398, https://doi.org/10.1007/s11250-011-9952-8.

[5] J. Zhang, J. Cao, M. Zhu, M. Xu, F. Shi, Loop-mediated isothermal amplification-lateral-flow dipstick (LAMP-LFD) to detect Mycoplasma ovipneumoniae, World J. Microbiol. Biotechnol. 35 (2) (2019) 31, https://doi.org/10.1007/s11274-019-2601-5.

[6] G.C. Weiser, M.L. Drew, E.F. Cassirer, A.C. Ward, Detection of Mycoplasma ovipneumoniae and M. arginini in bighorn sheep using enrichment culture coupled with genus- and species-specific polymerase chain reaction, J. Wildl. Dis. 48 (2) (2012) 449–453, https://doi.org/10.7589/0090-3558-48.2.449.

[7] Q. Chen, L. Zhang, F. Jiang, B. Wang, T. Lv, Z. Zeng, W. Wu, S. Sun, MnO_2 microsphere absorbing Cy5-labeled single strand DNA probe serving as powerful biosensor for effective detection of mycoplasma ovipneumoniae, Sensor. Actuator. B Chem. 244 (2017) 1138–1144, https://doi.org/10.1016/j.snb.2017.01.104.

[8] T. Ramon-Marquez, A.L. Medina-Castillo, A. Fernandez-Gutierrez, J.F. Fernandez-Sanchez, A novel optical biosensor for direct and selective determination of serotonin in serum by Solid Surface-Room Temperature Phosphorescence, Biosens. Bioelectron. 82 (2016) 217–223, https://doi.org/10.1016/j.bios.2016.04.008.

[9] J. Chen, J. Zhang, Y. Guo, J. Li, F. Fu, H.H. Yang, G. Chen, An ultrasensitive electrochemical biosensor for detection of DNA species related to oral cancer based on nuclease-assisted target recycling and amplification of DNAzyme, Chem. Commun. 47 (28) (2011) 8004–8006, https://doi.org/10.1039/c1cc11929j.

[10] M. Chen, C. Hou, D. Huo, H. Fa, Y. Zhao, C. Shen, A sensitive electrochemical DNA biosensor based on three-dimensional nitrogen-doped graphene and Fe_3O_4 nanoparticles, Sens. Actuators BChemical. 239 (2017) 421–429, https://doi.org/10.1016/j.snb.2016.08.036.

[11] H. Wu, C.J. Lee, H. Wang, Y. Hu, M. Young, Y. Han, F.J. Xu, H. Cong, G. Cheng, Highly sensitive and stable zwitterionic poly(sulfobetaine-3,4-ethylenedioxythiophene) (PSBEDOT) glucose biosensor, Chem. Sci. 9 (9) (2018) 2540–2546, https://doi.org/10.1039/C7SC05104B.

[12] N. Hui, X. Sun, Z. Song, S. Niu, X. Luo, Gold nanoparticles and polyethylene glycols functionalized conducting polyaniline nanowires for ultrasensitive and low fouling immunosensing of alpha-fetoprotein, Biosens. Bioelectron. 86 (2016) 143–149, https://doi.org/10.1016/j.bios.2016.06.028.

[13] S. Moraes Silva, R. Tavallaie, L. Sandiford, R.D. Tilley, J.J. Gooding, Gold coated magnetic nanoparticles: from preparation to surface modification for analytical and biomedical applications, Chem. Commun. 52 (48) (2016) 7528–7540, https://doi.org/10.1039/c6cc03225G.

[14] G. Jie, J. Ge, X. Gao, C. Li, Amplified electrochemiluminescence detection of CEA based on magnetic Fe_3O_4@Au nanoparticles-assembled Ru@SiO_2 nanocomposites combined with multiple cycling amplification strategy, Biosens. Bioelectron. 118 (2018) 115–121, https://doi.org/10.1016/j.bios.2018.07.046.

[15] Q. Han, X. Shen, W. Zhu, C. Zhu, X. Zhou, H. Jiang, Magnetic sensing film based on Fe_3O_4@Au-GSH molecularly imprinted polymers for the electrochemical detection of estradiol, Biosens. Bioelectron. 79 (2016) 180–186, https://doi.org/10.1016/j.bios.2015.12.017.

[16] N. Hui, X. Sun, S. Niu, X. Luo, PEGylated polyaniline nanofibers: antifouling and conducting biomaterial for electrochemical DNA sensing, ACS Appl. Mater. Interfaces 9 (3) (2017) 2914–2923, https://doi.org/10.1021/acsami.6b11682.

[17] Y. Wang, M. Cui, M. Jiao, X. Luo, Antifouling and ultrasensitive biosensing interface based on self-assembled peptide and aptamer on macroporous gold for electrochemical detection of immunoglobulin E in serum, Anal. Bioanal. Chem. 410 (23) (2018) 5871–5878, https://doi.org/10.1007/s00216-018-1201-9.

[18] H. Ye, Y. Xia, Z. Liu, R. Huang, R. Su, W. Qi, L. Wang, Z. He, Dopamine-assisted deposition and zwitteration of hyaluronic acid for the nanoscale fabrication of low-fouling surfaces, J. Mater. Chem. B 4 (23) (2016) 4084–4091, https://doi.org/10.1039/C6TB01022A.

[19] X. Cao, B. Zhu, X. Zhang, H. Dong, Polymyxin B immobilized on cross-linked cellulose microspheres for endotoxin adsorption, Carbohydr. Polym. 136 (2016) 12–18, https://doi.org/10.1016/j.carbpol.2015.09.012.

[20] Z. Du, F. Shi, D. Liu, H. Ye, M.M. Surhio, J. Li, M. Ye, Anticoagulant activity of a sulfated Lachnum polysaccharide in mice with a state of hypercoagulability, Bioorg. Med. Chem. Lett 26 (22) (2016) 5550–5556, https://doi.org/10.1016/j.bmcl.2016.09.079.

[21] X. Wu, Q. Huang, Y. Mao, Y. Wang, Q. Hu, H. Wang, X. Wang, Sensors for determination of uranium: a review, Trac. Trends Anal. Chem. 118 (2019) 89–111, https://doi.org/10.1016/j.trac.2019.04.026.

[22] N.Z. Liu, J.Y. Song, Y.W. Lu, J.J. Davis, F.X. Gao, X.L. Luo, Electrochemical aptasensor for ultralow fouling cancer cell quantification in complex biological media based on designed branched peptides, Anal. Chem. 91 (13) (2019) 8334–8340, https://doi.org/10.1021/acs.analchem.9b01129.

[23] T. Yan, L. Zhu, H. Ju, J. Lei, DNA-Walker-Induced allosteric switch for tandem signal amplification with palladium nanoparticles/metal-organic framework tags in electrochemical biosensing, Anal. Chem. 90 (24) (2018) 14493–14499, https://doi.org/10.1021/acs.analchem.8b04338.

[24] D. Zhao, G. Yu, K. Tian, C. Xu, A highly sensitive and stable electrochemical sensor for simultaneous detection towards ascorbic acid, dopamine, and uric acid based on the hierarchical nanoporous PtTi alloy, Biosens. Bioelectron. 82 (2016), https://doi.org/10.1016/j.bios.2016.03.074.

[25] X. He, H. Han, L. Liu, W. Shi, X. Lu, J. Dong, W. Yang, X. Lu, Self-assembled microgels for sensitive and low-fouling detection of streptomycin in complex media, ACS Appl. Mater. 11 (14) (2019) 13676–13684, https://doi.org/10.1021/acsami.9b00277.

[26] S. Xie, J. Ye, Y. Yuan, Y. Chai, R. Yuan, A multifunctional hemin@metal–organic framework and its application to construct an electrochemical aptasensor for thrombin detection, Nanoscale 7 (43) (2015) 18232–18238, https://doi.org/10.1039/C5NR04532K.

[27] M. Baghayeri, H. Veisi, M. Ghanei-Motlagh, Amperometric glucose biosensor based on immobilization of glucose oxidase on a magnetic glassy carbon electrode modified with a novel magnetic nanocomposite, Sensor. Actuator. B Chem. 249 (2017) 321–330, https://doi.org/10.1016/j.snb.2017.04.100.

[28] G. Ding, S. Xie, Y. Zhu, Y. Liu, L. Wang, F. Xu, Graphene oxide wrapped Fe3O4@Au nanohybrid as SERS substrate for aromatic dye detection, Sens. Actuators BChemical. 221 (2015) 1084–1093, https://doi.org/10.1016/j.snb.2015.07.074.

[29] M. Freitas, M. Sá Couto, M.F. Barroso, C. Pereira, N. de-los-Santos-Álvarez, A.J. Miranda-Ordieres, M.J. Lobo-Castañón, C. Delerue-Matos, Highly monodisperse Fe3O4@Au superparamagnetic nanoparticles as reproducible platform for genosensing genetically modified organisms, ACS Sens. 1 (8) (2016) 1044–1053, https://doi.org/10.1021/acssensors.6b00182.

[30] L. Yu, Y. Zhang, R. Chen, D. Zhang, X. Wei, F. Chen, J. Wang, M. Xu, A highly sensitive resonance light scattering probe for Alzheimer's amyloid-beta peptide based on Fe3O4@Au composites, Talanta 131 (2015) 475–479, https://doi.org/10.1016/j.talanta.2014.07.067.

[31] S. Barreda-García, M.J. González-Álvarez, N. de-los-Santos-Álvarez, J.J. Palacios-Gutiérrez, A.J. Miranda-Ordieres, M.J.J.B. Lobo-Castañón, Attomolar quantitation of Mycobacterium tuberculosis by asymmetric helicase-dependent isothermal DNA-amplification and electrochemical detection, Biosens. Bioelectron. 68 (2015) 122–128, https://doi.org/10.1016/j.bios.2014.12.029.

[32] C. Su, Z. Li, D. Zhang, Z. Wang, X. Zhou, L. Liao, X. Xiao, A highly sensitive sensor based on a computer-designed magnetic molecularly imprinted membrane for the determination of acetaminophen, Biosens. Bioelectron. 148 (2020) 111819, https://doi.org/10.1016/j.bios.2019.111819.